Sequence Specific Phosphopeptide Enrichment of ZAP-70 regulatory motifs using epitope-imprinted polymer complements

Anıl Incel[1†], Sudhirkumar Shinde,[1,3†*] Ignacio A. Diez[2], Maria M. Stollenwerk[1], Ole N. Jensen[2] and Börje Sellergren[1,3*]

Abstract.

Immunoaffinity enrichment based on antipeptide antibodies coupled to mass spectrometry-based identification and quantification (immuno-MS) is a promising approach to translate proteomics to clinical assays with diagnostic value. This is linked to precision cancer medicine, where immuno-MS based studies of protein phosphorylation dependent-signalling states of cells enable pathway targeted therapies and response monitoring to be developed. Clinically robust methods depend on the availability of high quality phosphopeptide antibodies but these rarely meet the stringent demands on reproducibility, robustness, availability and peptide specificity. We here show that polymer-based "plastic antibodies" prepared by molecular imprinting could play this role. Focusing on the Tyr-492 and Tyr-493 kinase regulatory motif of the SH2 domain in ZAP-70, a critical mediator in T-cell receptor signalling, we show that MIPs can be easily generated to recognize corresponding mono- or di-phosphorylated tryptic peptides in a highly specific manner. The polymers bound their complementary phosphorylated decapeptides with Kd:s in the low μM range in both low aqueous proteomics media and aqueous buffers. Moreover, only minor cross-reactivity was

observed for phosphopeptide variants with identical amino acid sequence. Proving their practical value, we demonstrate their use for sequence specific phosphopeptide enrichment from extracts of Jurkat T-cells stimulated to induce protein phosphorylation at either of the two regulatory sites of ZAP-70. We expect the approach to be broadly applicable paving the way for robust, low-cost multiplex phosphopeptide assays.

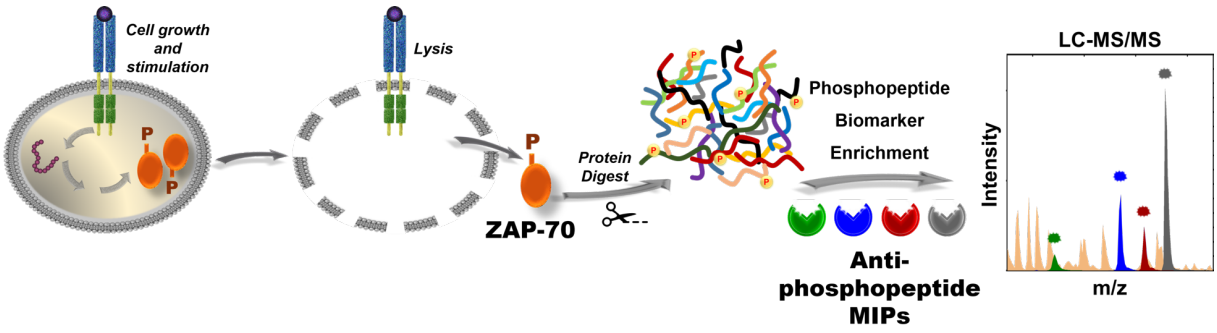

TOC Graphics

---

[1]Department of Biomedical Science, Faculty of Health and Society, Malmö University, 205 06 Malmö, Sweden

[2]Department of Biochemistry and Molecular Biology and VILLUM Center for Bioanalytical Sciences, University of Southern Denmark, DK-5230 Odense M, Denmark

[3]Faculty of Chemistry, Technical University of Dortmund, 44227 Dortmund, Germany

[†]These authors contributed equally

[*]Corresponding Author. E-mail: borje.sellergren@mau.se

Introduction

Protein phosphorylation is a reversible post-translational modification (PTM) influencing protein localization, protein-protein interactions, and intracellular protein activities. This PTM is the key chemical signal in complex molecular networks and pathways, which controls gene expression and in turn cell behavior in response to extracellular signals.[1-4] Dysfunctions in the signalling network commonly involves enhanced kinase activity and abnormal phosphorylation is thus a common hall mark of several diseases with cancer as a notable example.[5] In spite of genetic alterations being the underlying cause for these defects, the direct identification and quantification of distinct protein phosphorylation events is needed to understand the disease driving mechanisms and in turn to tailor therapies at an individual level. This has spurred the development of functional phosphoproteomics, most frequently based on affinity-based phosphopeptide enrichment combined with advanced mass spectrometry (MS). This technique is capable of detection, sequencing and quantification of thousands of protein phosphorylation sites in large-scale experiments.[6-9]

In spite of the scalability, speed and sensitivity of current phosphoproteomics methods, robustness is typically insufficient for its routine use for instance in clinical settings.[10,11] This may be addressed by targeted phosphoproteomics involving site-specific phosphopeptide enrichment and selective MS readout techniques.[5,12,13] This in turn paves the way for routine multiplex biomarker quantifications, a requirement for the technique to be useful for routine use. Immunobased phosphopeptide enrichments have in this context emerged as one enabling tool allowing deep profiling of multiple phosphopeptides in a reproducible and robust assay format.[5] This is offset by current limitations in delivering antibodies fulfilling high specificity, high affinity as well as high reproducibility and the highly variable

immunogenicity of phosphopeptides per se.[12] To compensate for this lack of affinity tools, we set out to investigate whether molecular imprinting technology[14-20] could fill this gap.

A molecularly imprinted polymer (MIP) refers to a synthetic polymer with templated binding or catalytic sites.[21] MIPs are typically prepared by conventional network polymerization in the presence of a template serving the dual role of preorganizing individual monomers and as a mold for inducing shape complementary binding sites. Removal of the template result in a MIP exhibiting antibody-like recognition behavior with nanomolar, or higher, affinities for the template or targets with template substructures.[22,23] These binders are robust, resist denaturing solvents, high temperatures and can be reproducibly and cost-effectively produced. Hence, they are potentially useful as antibody substitutes in protein and glycan detection strategies. MIPs targeting protein PTMs have in this context emerged as a promising alternative to established affinity reagents.[24-29 30 31-33] For instance, efficient amino acid side chain specific enrichment of tryptic peptides from cell lysates or complex protein digests have been demonstrated for phosphotyrosine[31], phosphoserine[27] and most recently labile phosphohistidine PTMs[33]. The design of these MIPs relies on the use of neutral urea-based host monomers with tunable affinity for oxyanions such as carboxylates and phosphates. Exploiting the ability of divalent phosphate to coordinate two such groups, MIPs can be prepared featuring cleft-like receptors with tight affinity for the template or target epitopes.[25,34] In contrast to most other phosphopeptide enrichment techniques, these receptors are charge neutral and therefore less biased towards peptides comprising other charged amino acid residues, such as Glu and Asp.[27]

To apply this technique to the enrichment of specific phosphopeptides we focused on Zeta-chain associated protein kinase 70 kDa (ZAP-70), a well-characterized protein playing a central role as mediator in the T-cell receptor (TCR) signalling cascade. [35,36 37-39] ZAP-70 is inactive

cytosolic tyrosine kinase which associates with immunoglobulin tyrosine-based activation motifs (ITAMs) on the transmembrane TCR via two SH2 domain modules.[35] These are connected to the kinase domain via a flexible interdomain **(Scheme 1a)**.

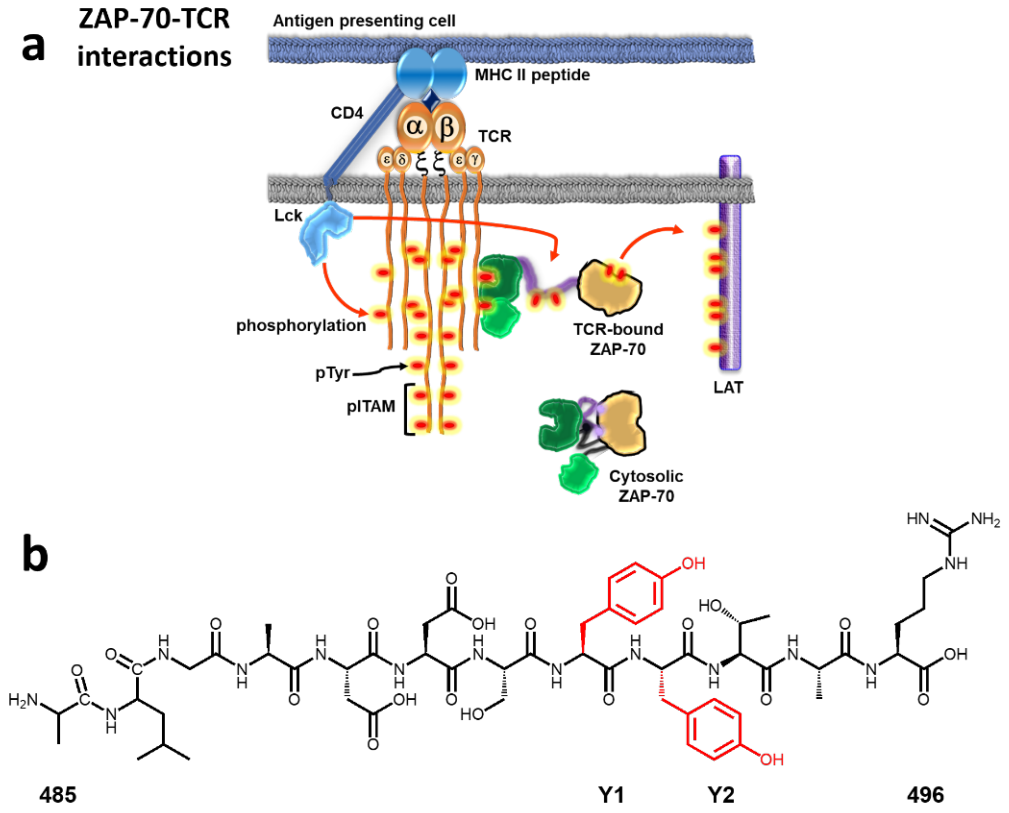

Scheme 1. **a,** Schematic drawing of the early stages of TCR signaling comprising the activation of ZAP-70 by phosphorylation at Y492 and Y493. The TCR interacts with a peptide/MHC (major histocompatibility complex) on antigen-presenting cells. This leads to attraction of the transmembrane co-receptor CD4 whose intracellular domains thereby associate with the Src family kinase Lck. Lck thereby catalyze phosphorylation of the ITAMs which in turn leads to recruitment of cytosolic ZAP-70 via SH2 domain association. **b,** Sequence of amino acids 485-496 of the ZAP-70 kinase domain.

ITAM association is suggested to free up tyrosine residues Y315 and Y319 of the interdomain facilitating their phosphorylation.[40] This leads to recruitment of other signalling molecules and renders the enzyme catalytically active. [41] The kinase activity is further controlled by two juxtaposed tyrosine residues in the kinase domain, Y492 and Y493, acting as negative and positive kinase activity regulators respectively **(Scheme 1b)**.[42-44] ZAP-70 overexpression and hyper-phosphorylation is linked to Chronic Lymphocytic Leukemia (CLL) highlighting the need for sensitive assays to monitor the relative abundance of the above phosphorylation sites. [39]

To address this need we set out to design MIPs capable of specific capture and enrichment of these targets. Based on our stoichiometric imprinting approach[45] we here show that MIP complements can be tailored to recognize each of the four phosphorylated and non-phosphorylated forms of the Y492/Y493 motif. These MIPs were used for direct enrichment of phosphopeptides from tryptic digests of proteins extracts from stimulated Jurkat T-cells setting new limits for the achievable precision of imprinting and its compatibility with protein phosphorylation assays in biochemistry and cell biology.

Results and discussion

MIP preparation and characterization

Stoichiometric imprinting relies on the use carefully designed functional monomers and templates that quantitatively associates in an appropriate solvent to form defined monomer-template complexes.[46] We previously showed that aryl-phosphonates and -phosphates strongly associate (Ka>>1000 M^{-1}) with urea monomer 1 in aprotic media to form higher order complexes.[25,34] Complexation is driven by hydrogen bonding with the urea group of 1 acting as a potent hydrogen bond donor and the phosphate monoanion or dianion as the acceptor leading to cyclic hydrogen bonded structures reflected in enhanced solubility behaviour **(Fig. S1)**. The complex stoichiometry is given by the phosphate ionization state with the monoanion and dianion promoting the formation of template:monomer 1:1 and 1:2 complexes respectively. To adapt this system to the ZAP-70 epitopes we first prepared the peptides in **Scheme 2a** by manual solid-supported synthesis using standard Fmoc chemistry **(Table S1-S2)**.[47] All peptides were obtained in acceptable yields (≥60 %) and purity (≥95%) based on LC-MS, ^{1}H-, ^{13}C- and ^{31}P-NMR characterization **(Fig S2-13)** and were transferred to bis-tetrabutylammonium salts prior to imprinting.

Preparation of the MIPs followed in large previously reported protocols using 1,3-diarylurea monomer 1 added in a twofold excess with respect to each peptide-phosphate group and with PETA as a hydrophilic crosslinker **(Scheme 2b, Table S3).**[33,34]

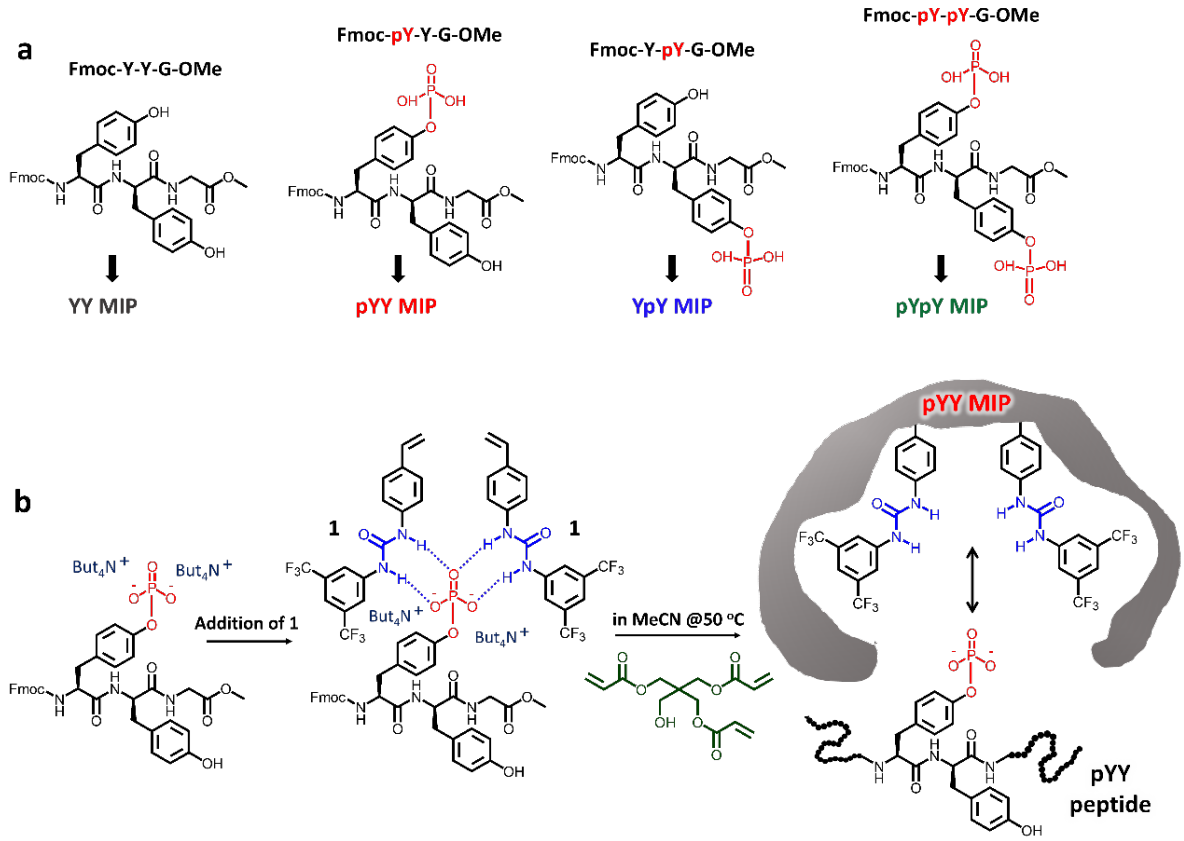

Scheme 2 | Synthesis of Imprinted Polymers. a, Structure of templates. **b**, procedure used for preparing MIP complements to the phosphorylated isomers of the ZAP-70 $Y^{492}Y^{493}$ motif.

Free radical polymerization was conducted with the initiator, monomers and templates dissolved in dry acetonitrile. The polymer monoliths were crushed and sieved to isolate a 25-36 µm particle-size fraction, followed by template removal by acid treatment. This led to a minimum template recovery of ca 90% resulting in a nominal capacity assuming 100% site occupancy of 15 µmol/g **(Fig. S14)**. Morphology and structural characterization were thereafter performed by scanning electron microscopy (SEM) **(Fig. S15)**, thermal gravimetric analysis (TGA) **(Fig. S16)**, and Fourier-transform infrared spectroscopy (FTIR) **(Fig. S17)**. Meanwhile, the Thermogravimetric analysis (TGA) resulted in weight loss curves typical for

highly cross-linked networks with onset above 200 °C and complete weight loss obtained at 450 °C. Moreover, the transmission FTIR spectra showed all characteristic bands with no apparent differences between the polymers. Overall, the data indicate a high monomer conversion and no apparent physical or chemical differences between the polymers.

Phosphopeptide binding studies

Imprinting effects were assessed by competitive binding assays by incubating the MIPs in equimolar peptide mixtures in different acetonitrile/water mixtures or aqueous buffers. First, we probed the polymer's ability to recognize their templates in an acetonitrile rich solvent system. This compensates for network solvation effects on recognition and is the standard gauge of the polymer's memory for their templates. [17] As seen in **Fig. S18** the phosphopeptide imprinted polymers each recognized their complementary templates with selectivity factors ($B_{template}/B_{competitor}$) with respect to the other templates exceeding two. The nonphosphorylated peptide meanwhile was not recognized by neither of the MIPs reflecting the lack of strong interactions with 1. Encouraged by this precise discrimination we went on to probe binding of phosphorylated forms of the ZAP-70 487-496 epitope **(Fig. 1)**. The four MIPs were hence incubated in acetonitrile/water or aqueous buffers containing the four decapeptides: nonphosphorylated YY, monophosphorylated pYY and YpY and diphosphorylated pYpY. **Fig. S19-20** show the specific uptakes of all peptides and **Fig. 1** the corresponding stacked selectivity factors in the different solvents. **Fig. S19** shows that the polymers also crossreact with the complementary decapeptides but that this effect is strongly solvent dependent. In the buffered acetonitrile/water mixtures only in 90% acetonitrile buffered with TFA is this effect strongly manifested **(Fig. 1a, Fig. S19a)**. Under these conditions more than 90% of the complementary peptides were bound with selectivity factors all

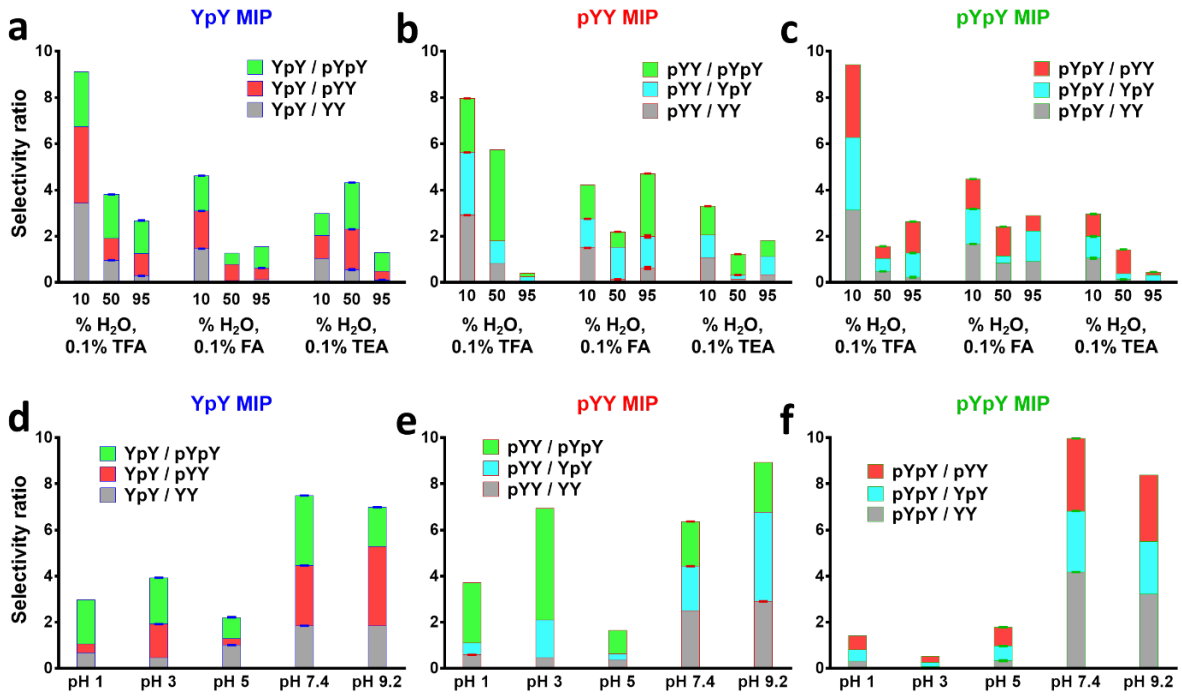

Fig. 1 | The phoshopeptide selectivity ratio of imprinted polymers towards deca-peptides. a-c, Results from equilibrium binding tests (n=3) to probe phosphopeptide selectivity as a function of water content in acetonitrile/water mixtures or **d-f**, buffer pH. The selectivity factor was determined as the % bound target over nontarget peptide (Fig. S19-20) as defined by the MIP design. pYpY = GADDS**pYpY**TAR, pYY = GADDS**pYY**TAR, YpY = GADDS**YpY**TAR, and YY = GADDS**YY**TAR.

exceeding 2. The discrimination was lost when replacing the strong acid TFA with the weaker acid (FA) or basic (TEA) modifiers. Meanwhile, increasing the aqueous content completely suppressed binding of the peptides. Binding tests using aqueous buffers showed that both uptake and selectivity depended strongly on the buffer pH. Hence, whereas binding of the peptides was elevated in low pH 1 and pH 3 buffers **(Fig. S20a, b)** it dropped overall with increasing pH **(Fig. S20c-e)**. At low pH, binding increased inversely with the number of phosphate groups of the peptide with YY displaying the strongest binding. This trend was no longer present at pH 5, although still with no imprint related discrimination to be seen. On the contrary, at neutral and basic pH, the MIPs specifically recognized their peptide complements, an effect seen most clearly in **Fig. S20d** and **Fig. 1d-f**. The above observations can be understood when taking a closer look at the peptide ionization states in the different buffers

(Table 1) and ionic strength effects. In the acetonitrile/water media **(Fig. S19, Fig. 1a-c)** the acidic modifiers TFA and FA reduces the charge of the phosphopeptides, while leaving the phosphate groups partly ionized for interacting with the urea N-H hydrogen bond donors. This facilitates their interactions with the templated sites explaining the pronounced phosphosite selectivities observed. This contrasts with results obtained with the basic modifier TEA, which renders all peptides multiply negatively, charged and strongly solvated. In addition, nonspecific effects due to the three carboxylic acid groups contribute to overall enhanced binding. In the aqueous buffers the binding dependence on the ionization state show clear trends. At pH 1, only the terminal amino acids are charged whereas the acidic side chains are protonated (pYpY being a possible exception) and charge neutral rendering all peptides an equal +2 charge. At pH 3, pTyr sites of the phosphopetides are ionized reducing the charge of the latter in comparison with the nonphosphorylated peptide. The latter, carrying a positive net charge, is still tightly bound. At pH 5, which is situated between the pKa of the Asp side chains and the pKa2 of the phosphotyrosines, the phosphate groups are only partially charged with only one H-bond acceptor free to interact with the MIP sites. Increasing pH from 5 to 7.4 however transforms the phosphate groups to dianions i.e., more potent hydrogen bond acceptors, manifested in a pronounced target discrimination. The effect prevails in the more basic buffer although less pronounced.

Table 1. Net charge of the ZAP-70 decapeptides[48] versus buffer pH.

Buffer	YY[a]	YpY/pYY[a]	pYpY[a]
pH **1**	2	2	2
pH **3**	1	0	–1
pH **5**	–1	–2	–3
pH **7.4**	–1	–3	–5
pH **9.2**	–1	–3	–5
TFA	2	1	0
FA	2	1	0
TEA	-2	-4	-6

YY[a] – GADDS**YY**TAR, YpY/pYY[a] – GADDS**YpY**TAR/ GADDS**pYY**TAR and pYpY[a] – GADDS**pYpY**TAR

The recognition effects observed in MeCN/water: 90/10 and neutral buffer led us to investigate the corresponding binding energy distribution in more detail.

Adsorption isotherms and binding parameters

The binding-energy distributions of the phospho-peptide targeting polymers were determined from single-component adsorption isotherms under static conditions. The binding data corresponding to the peptides binding to each MIP in 90% MeCN + 0.1% TFA and in HEPES buffer pH=7.4 are plotted in **Fig. 2 and Fig. S21**.

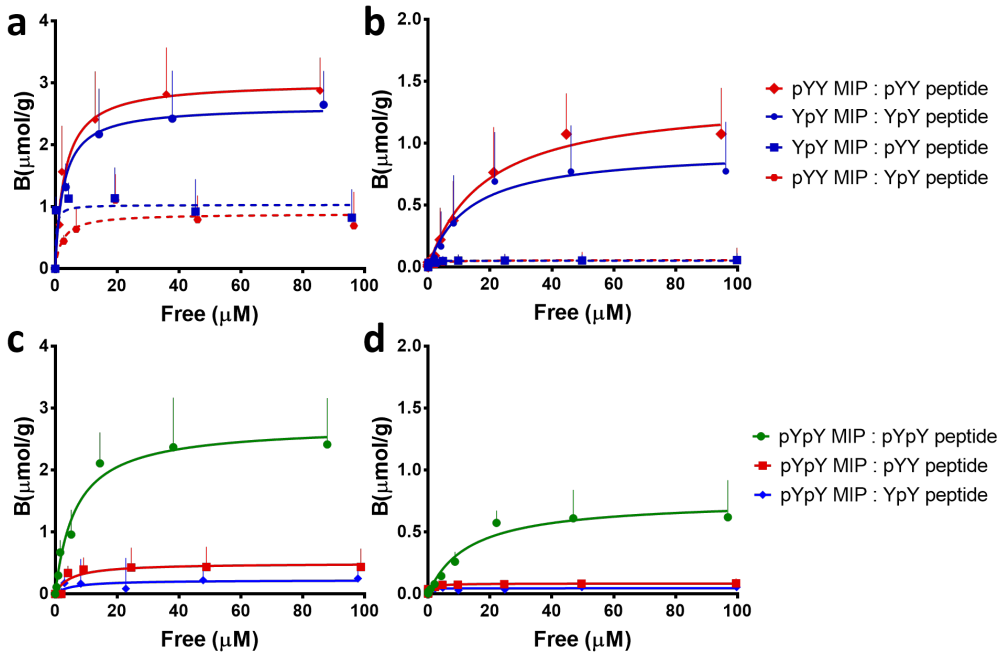

Figure 2 | Equilibrium binding isotherms of phospho-peptide targeting polymers incubated with indicated model peptides in. **a,** and **c**, MeCN/water: 90/10 (0.1% TFA). **b,** and **d**, HEPES buffer pH 7.4. pYY = GADDS**pYY**TAR, YpY = GADDS**YpY**TAR and pYpY = GADDS**pYpY**TAR.

In agreement with the initial peptide binding tests, the MIPs preferentially bound their phosphopeptide complement with a strong ability to discriminate against their structural analogs. Meanwhile, binding to the MIP targeting the non-phosphorylated peptide (YY MIP) was low for all peptides. Fitting the binding data with the Langmuir mono-site binding model resulted in the binding parameters given in **Table S4**. Overall, the polymers exhibited stronger

affinity for the peptides in the acetonitrile rich medium with saturation capacities (Bmax) for the peptide complements reaching 2.5-3 μmol/g and for the noncomplements ca 1 μmol/g for the pYY- and YpY- MIPs and 0.5 μmol/g for the pYpY MIP **(Table S4)**. The pronounced specificities were accompanied by dissociation constants K_D in the single digit μM range. Although this indicates a lower affinity than phosphoprotein antibodies the steep initial slope of the binding curve indicate presence of sites with higher affinity. Even more striking were the MIPs binding performance in the pH 7.4 buffer. In spite of the slightly lower affinity, the binding specificity shown by all phosphopeptide MIPs was absolute. For instance, the pYY MIP bound the pYY peptide but showed complete rejection of the YpY peptide and vice versa **(Fig. 2b)**. To investigate whether the pronounced discrimination prevailed in complex matrices we went on to peptide enrichment tests.

Enrichment of spiked phosphorylated ZAP-70 deca-peptides from protein digests

To check whether the pronounced phosphotyrosine peptide recognition and discrimination prevailed in biological samples we decided to stepwise increase the protein sample complexity. First, we performed spike-in experiments of a mixture of three of the model peptides (YY, YpY and pYpY or YY, pYY, and pYpY mixtures – each at spiking level: 1:5) in a digest of BSA and β-casein followed by ZAP-70 MIPs enrichments. The SPE flow-through (FT), wash (W) and elution (E) fractions were screened by MALDI-TOF MS, resulting in the spectra shown in **Fig. S22**. With most of the BSA and β-casein digest peptides found in the FT and W fractions, it is noted a significant reduction of sample complexity in the E fractions. The mass spectra of the fractions before and after YY-MIP based enrichment test are shown in **Fig. S22d**. Mass signals of all spiked peptides are found in the FT and W fractions whereas none in the E fraction. However, a different picture emerged from the spectra corresponding to the YpY-,

pYY- and pYpY- MIP based enrichment fractions **(Fig. S22a-c)**. In the enrichment using the YpY-MIP where YY, YpY, and pYpY peptides were spiked in the digest, the E fraction now revealed one single signal with a m/z matching the target YpY peptide (m/z = 1198.10) **(Fig. S22a)**. Likewise, the pYY-MIP based enrichment, where YpY was spiked instead of pYY, led to a similar result **(Fig. S22b)**. Targetting the doubly phosphorylated peptide, the pYpY-MIP was tested with the same spiked digest as used in YpY-MIP enrichment. Again, the target peptide was specifically enriched on this MIP as shown by the appearance of a single signal with a m/z matching pYpY (m/z = 1278.09) **(Fig. S22c)**. Meanwhile YpY was detected in both the FT and W fractions. In all the aforementioned enrichments, the non-phosphorylated peptide YY (m/z= 1118.11) was mainly recovered in the FT fractions.

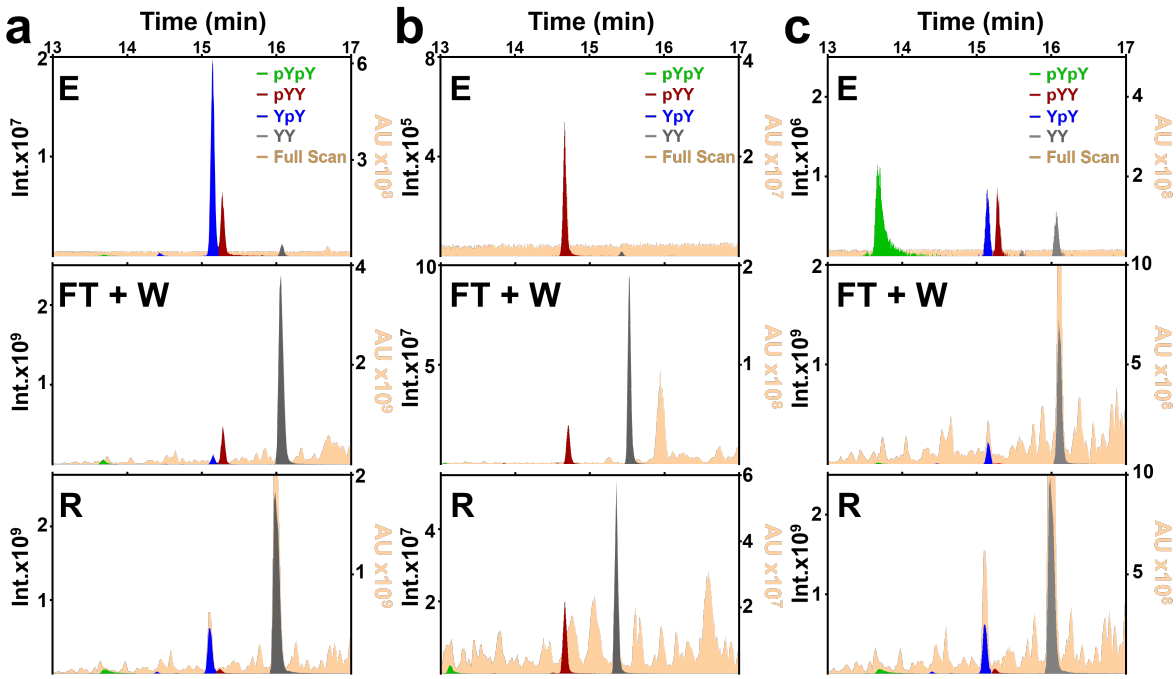

Fig. 3 | Extracted LC-MS/MS profiles of highlighting spiked ZAP-70 peptides (indicated in colors) corresponding to fractions in the enrichment. a, YpY-, **b**, pYY-, **c**, pYpY-MIP. Up to down E = Elution, FT + W = flow-through + washing, R = reference fractions. The spiked peptides are pYpY = GADDS**pYpY**TAR (green), YpY = GADDS**YpY**TAR (blue), pYY = GADDS**pYY**TAR (red), and YY = GADDS**YY**TAR (gray). The light pink chromatogram in the background stands for full chromatogram. The left y-axis shows intensity of spiked peptides, the right y-axis refers for the intensity of full chromatogram. The spiking level is 1:10 for target:non-target peptides.

Increasing sample complexity further, we tested a 12-protein digest in the same manner as above but with the model peptides spiked at the 1/10, 1/100, and 1/1000 levels. Fractions were collected from each step and analyzed by nanoliter flow LC-MS/MS (Orbitrap mass analyzer). **Fig. 3** (spiking level is 1:10) and **Fig. S23** (spiking level is 1:100) show the extracted ion chromatograms corresponding to the pre-enrichment control (reference, R) sample and the post-enrichment (flow through + wash, FT+W and elution, E) fractions.

The MIP sample processing protocol effectively removed background signals at both spiking levels as judged from the LC-UV chromatograms (light pink) of the elution fractions (E) compared to reference (R) **(Fig. 3)**. Meanwhile highly specific extractions of the target peptides were evident but with slight variations depending on the phosphorylation pattern and spiking level. Tests using the YpY (YY, YpY, and pYpY peptides spiked in enrichment) and pYY (YY, pYY, and pYpY peptides spiked in enrichment) MIPs, targeting the monophosphorylated forms, cleanly extracted their targets while completely **(Fig. 3)** or partially **(Fig. S23)** rejecting the nonphosphorylated and diphosphorylated peptides, albeit with breakthrough noted for pYY. [48]

The relative abundances of the spiked peptides **(Fig. S24)** confirm the results in Fig. 3 and Fig. S23 **(Fig. S24a, b)** while revealing other more subtle effects. First considering the SPE results using the digest spiked with pYpY, YpY and YY (left graphs in Fig. S24). The enrichments of the target peptides (YpY and pYpY) on their MIP complements, reflected in their relative abundance in the elution fractions, decreases with increasing dilution but still with a noticeable target selectivity. This contrasts with the experiments using the digest spiked with pYpY, pYY and YY (right graphs in Fig. S24). In this case, only pYY is selectively enriched whereas pYpY enrichment is noted only at the 1/10 spiking level. This suggests that pYY, in contrast to YpY, effectively competes with pYpY for interacting with the pYpY imprinted sites.

Detection of site-specific ZAP-70 phosphorylation in Jurkat leukemic T-cells

ZAP-70 protein tyrosine kinase is a prognostic factor in B cell chronic lymphocytic leukemia (B-CLL).[38] Its overexpression is related to the progress of the disease while aberrant phosphorylation of the protein is considered as a negative prognostic factor for the disease.[39,44] The above spike-in experiments show that MIPs can recognize both the number and position of phosphate groups in the ZAP-70 kinase regulatory motif. Thus, the question was whether this ability, selectivity and specificity would prevail when exposed to protein extracts from cell lysates.

To stimulate phosphorylation and expression of the protein we focused on Jurkat T-cells, a human leukemic T cell lymphoblast cell line. Our first goal was to investigate whether the cells could be selectively stimulated to express phosphorylation at either Y492, Y493 or at both positions. This would allow us to probe the efficiency of the MIPs to enrich their targets in competition with excess of the other isoforms. For this purpose, we applied different bio- and chemical stimuli known to up- or down- regulate phosphorylation at the two sites and verified the outcome by Western Blot analysis using anti ZAP-70 phospho-antibodies. After profiling and identification of the overexpressed ZAP-70 phosphoproteins, whole cell lysate digestion or in-gel proteolytic digestion of the protein was performed, and the digest analyzed or used for further enrichment experiments (**Fig. S25**).

For the stimulation, different regulators and their combinations were employed. An antibody targeting CD3, the upstream ZAP-70 recruiter in the TCR signalling cascade can be used to stimulate TCR signalling with increased phosphorylation activities.[49] Hydrogen peroxide is a reactive oxygen species, activating the response of extracellular receptor kinases via oxidative stress, which in turn initiates TCR signaling and activation of ZAP-70.[50] Finally, sodium pervanadate is an inhibitor of phosphotyrosyl protein phosphatases (PAP) and hence, it can

be used to generally boost protein phosphorylation.[51] The cells were stimulated using individual regulators or combinations of regulators as shown in **Fig. 4a** thereafter lysed and the lysate subsequently analysed by PAGE and WB using the anti-phospho ZAP 70 antibodies. Percent changes in band intensities revealed the relative expression levels of the two ZAP-70 proteins. First, we note that the non-stimulated cells feature constitutive hyperphosphorylation of Y493. This is in line with previous reports, showing that phosphorylation of Y493 is a positive regulatory mechanism required for activation of ZAP-70 and lymphocyte antigen receptor function.[42-44] Anti-CD3 stimulation slightly increased the Y493 phosphorylation compared to the basal level while Y492 phosphorylation remained unchanged. H_2O_2 stimulation alone caused a slight decrease of the Y493 phosphorylation, an effect reinforced in presence of anti-CD3 that also boosted Y492 phosphorylation. In contrast, stimulation with Na_2VO_4 alone or in combination with anti-CD3 caused a pronounced accumulation of phosphorylation at Y492, induced by the phosphatase inhibition, while the phosphorylation at Y493 remained indistinguishable from non-stimulated or anti-CD3-stimulated cells.

The catalytic kinase activity of ZAP-70 is known to depend on the mode of phosphorylation of the two-tyrosine residues Y492 and Y493 in the so-called activation loop.[42-44] Y493 phosphorylation leads to rearrangement of the activation loop, which frees up the catalytic center for further downstream signaling. On the other hand, Y492 phosphorylation has been invoked as a negative activity regulator. Indeed, phosphorylation on Y493 might follow by auto-phosphorylation of Y492.[42]

Having confirmed that phosphorylation of Y492 and Y493 can be selectively stimulated, we focused on cell lysates stimulated with anti-CD3 and anti-CD3 + H_2O_2 for the proteomics analysis.

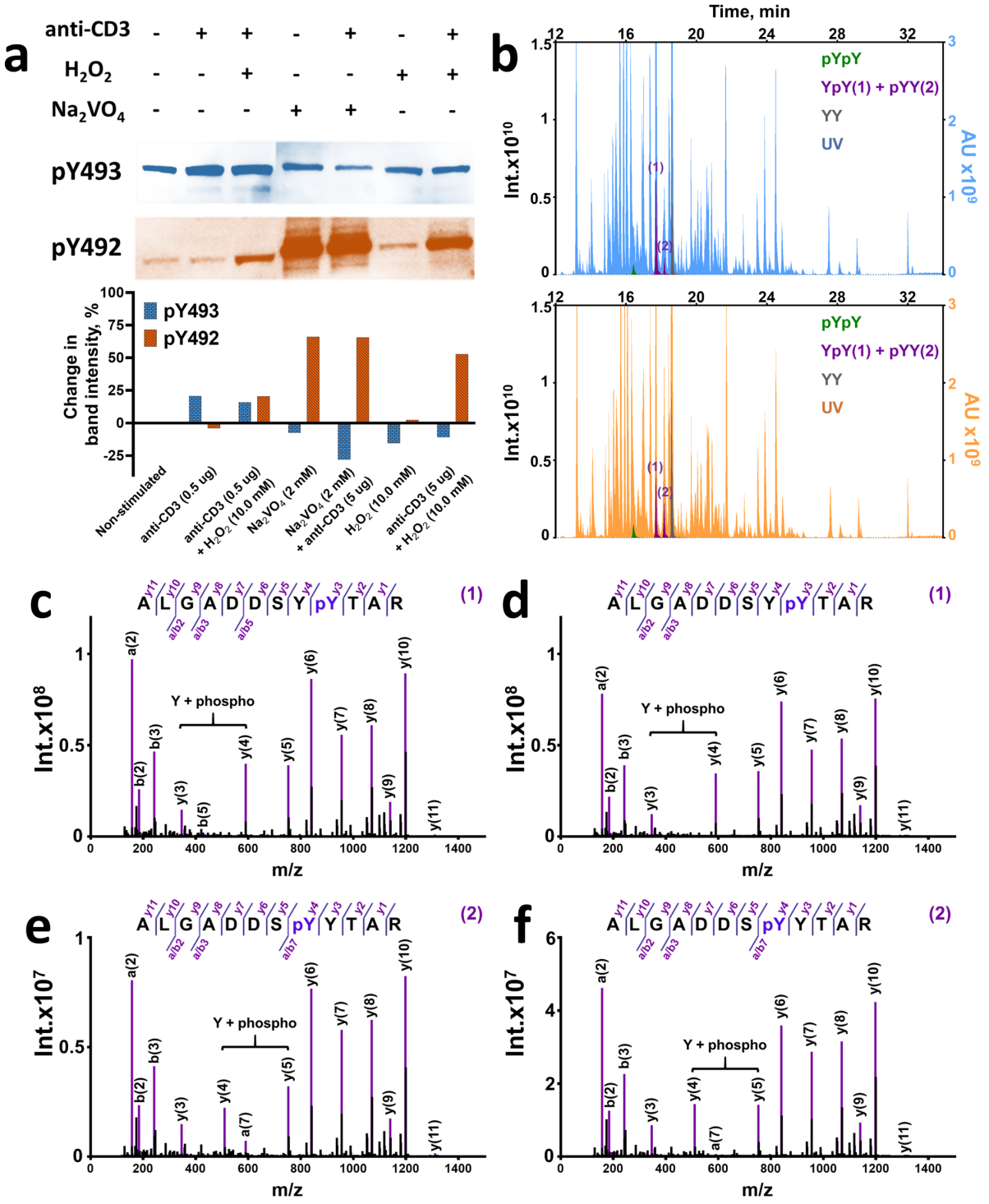

Fig. 4 | Characterization of Proteins and Peptides obtained by Jurkat leukemic T-cell line. a, Western blot analysis using anti-pY492 and anti-pY493 antibodies for identification of phosphoproteins. **b**, LC-MS/MS analysis of peptide mixture produced via in-gel digested ZAP-70 phosphoproteins after stimulation with anti-CD3 (top) or with a combination of anti-CD3 + H_2O_2 (bottom). The target phosphopeptides and non-phosphorylated counterpart are indicated pYpY = ALGADDS**pYpY**TAR (green) – RT: 16.3 min, YpY(1) = ALGADDS**YpY**TAR – RT: 17.8 min + pYY(2) = ALGADDS**pYY**TAR – RT: 18.2 min (purple), and YY = ALGADDS**YY**TAR – RT: 18.6 min (gray) (**b**). **c-f**, the MS/MS spectra derived from the fragmentation of ALGADDS**YpY**TAR (**c, d**) and ALGADDS**pYY**TAR (**e, f**) after stimulation with anti-CD3 (**c, e**) and after stimulation with anti-CD3 + H_2O_2 (**d, f**). RT: retention time.

Proteomic analysis of ZAP-70 protein digests of Jurkat T-cell lysates

The amino acid sequence of ZAP-70 is shown in **Table S6** and the list of possible short tryptic peptides of ZAP-70 YY including various phosphorylation states in the kinase domain in **Table S7**. For the identification of these and other endogenous phosphopeptides of ZAP-70 digests, proteins were first isolated by gel electrophoresis by cutting the polyacrylamide gel between 50 kDa and 75 kDa followed by in-gel proteolytic digestion as described in the experimental section. The sample complexity and peptide profiles of digested ZAP-70 phosphoproteins from anti-CD3 and anti-CD3+H_2O_2 stimulated cells were screened using LC-MS/MS (**Fig. 4b)**. All YY peptides could be identified in the chromatograms i.e. YY (gray, Mw 1302.5 g/mol), YpY (1) and pYY (2) (purple, Mw 1382.5 g/mol) and pYpY (green, Mw 1462.5 g/mol). Confident phosphorylation site localization of isobaric peptides was achieved by comparing their MS/MS fragmentation patterns (**Fig. 4c-f, Fig. S26**). Thus ALGADDS**YpY**TAR with characteristic y(4) ion at m/z = 590.2 (**Fig. 4c, e**) and ALGADDS**pYY**TAR with characteristic y(4) at m/z = 510.2 (**Fig. 4d, f**) verified presence of the pYY and YpY motifs, respectively.

While the intensities of YpY and YY were similar after both stimulations, the pYY intensity increased after the anti-CD3+H_2O_2 stimulation compared to the non-stimulated cells. Although this is in qualitative agreement with the WB results the pYY/YpY intensity ratio is markedly lower in the MS/MS compared to the WB analysis (**Fig. 4a**). This difference likely originates from a limited antibody specificity. We therefore compared the level of pYpY after the two stimulations and as expected, the pYpY signal increased in intensity after the anti-CD3 + H_2O_2 stimulation (**Fig. S26 c, d**). Crossreactivity of anti-p492 with pYpY could therefore account for the quantitative discrepancy between the MS/MS and WB analytical results.

Enrichment of ZAP-70 phosphopeptides from stimulated Jurkat T-cells

To test the ZAP-70 MIPs ability to enrich phoshopeptides from a complex cell lysate we first focused on the in-gel tryptic digests of the ZAP70 protein band obtained by SDS-PAGE. The LC-MS/MS profiles of the pre-enrichment (reference) and elution fractions are shown in **Fig. 5**. As in the spike in experiments, the overall peptide abundance was significantly lowered in the elution fractions (**Fig. 5, Fig. S27**) compared to the pre-enrichment and FT+W fractions (**Fig. S28**).

Focusing first on the target phosphorylated ZAP-70 peptides, the measured abundances of YpY and pYY in the pre-enrichment fractions agreed with the WB results. Thus, the YpY/pYY intensity ratio was significantly higher in the anti-CD3 (**Fig. 5a**) compared to the anti-CD3/H_2O_2 stimulated cell lysate (**Fig. 5b**) whereas the pYpY signal intensity was lower and the YY remained unchanged. Turning to the enrichment results we were pleased to see that the MIP specificity remained intact also in this native sample (Fig. 5). Hence, all target peptides were cleanly eluted with a near quantitative recovery and with intensity ratios mirroring the WB and MS/MS results, the latter appearing clearly when scrutinizing the relative abundancy graphs in Fig. S29. All in all, these data shows that phosphopeptide specific MIPs are compatible with direct target enrichment from lysate digests and that enrichment specificities can exceed those of antibodies.

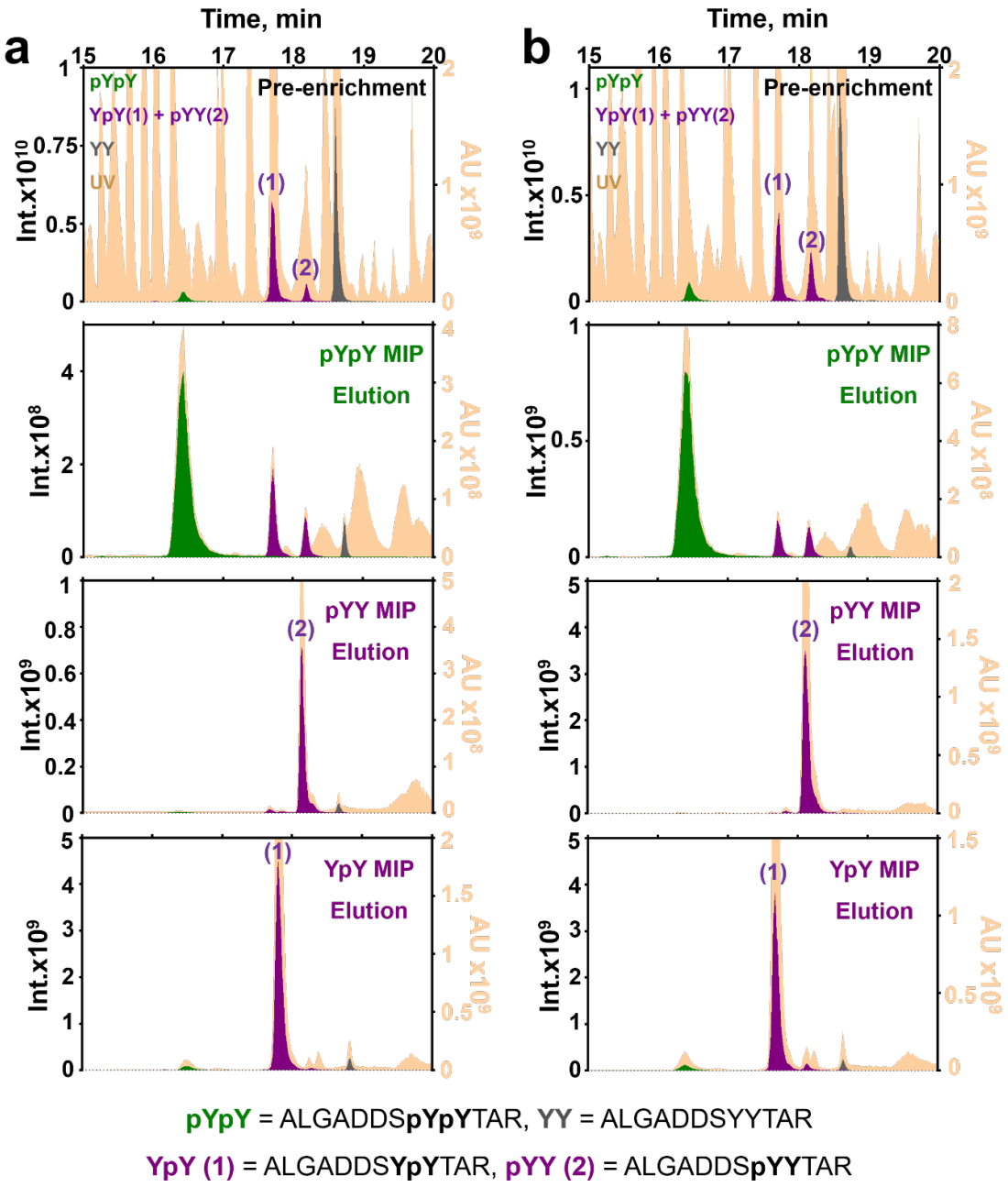

Fig. 5 | Extracted LC-MS/MS chromatogram highlighting ZAP-70 peptides (pYpY: ALGADDS**pYpY**TAR, green, YpY(1): ALGADDS**YpY**TAR, and pYY(2): ALGADDS**pYY**TAR, purple and YY: ALGADDSYYTAR, gray in color) corresponding to the pre-enrichment and elution fractions using **a**, Anti-CD3 stimulated/in-gel digested sample. **b**, Anti-CD3/H2O2 stimulated/in-gel digested sample. Up to down is pre-enrichments to elution fractions extracted from pYpY-, pYY-, and YpY- MIPs. (The range for relative abundance where all ZAP-70 peptides were eluted from 15 to 20 min).

Conclusions

Large-scale genomics, proteomics and metabolomics technologies have been used to find more precise predictive biomarkers for clinical applications. In this context an urgent need for robust affinity-based sample preparation techniques has emerged that can provide easy-to-use and reliable biomarker recovery, identification and detection. Protein phosphorylation analysis using mass spectrometry and applications of enrichment techniques such as IMAC and MOAC in particular is commonly restricted to generic enrichment of phosphorylated residues. Here we demonstrate that molecularly imprinted polymers provide a new dimension in offering the ability to tailor the enrichments towards specific amino acid modifications or peptide sequences. This may reveal hitherto unknown phosphorylation sites or offer a useful tool for targeted phosphoproteomics. We show here that sequence specific binders are capable of specific enrichment of the targeted pTyr peptides directly from in-gel digests of protein from cell lysates. To demonstrate the approach we focused on ZAP-70, a mediating kinase in the TCR signalling cascade with a phosphorylation state being a prognostic factor of Chronic Lymphocytic Leukemia (CLL). The results show that the MIP binders could cleanly enrich phosphopeptides corresponding to the regulatory motif of the ZAP-70 kinase domain. Notable features are the absolute discrimination of all phosphorylated forms of peptides featuring two juxtaposed tyrosines ($Y_{492}Y_{493}$), the high specificity and affinity for a doubly phosphorylated peptide and the high apparent recovery observed from native samples. This complements phosphospecific antibodies for this sequence motif that commonly exhibit undesirable crossreactivities. We foresee this kind of precision imprinting to be broadly applicable paving the way for robust, low-cost multiplex phosphopeptide assays compatible with clinical proteomics platforms.

Author Contributions

B.S. conceived and directed the project. A.I. wrote the first version of the manuscript. B.S., S.S., A.I., O.N.J. and I.A.D. designed the experiments, evaluated the data and contributed to writing of the final version of the manuscript. S.S. synthesized the templates, the first batch of MIPs and carried out initial polymer characterization. A.I. optimized and characterized the MIPs, designed and performed the cell stimulation protocol and protein expression analysis. I.A.D. performed all LC-MS/MS analysis and related data evaluation. O.N.J. supervised the LC-MS/MS experiments, performed data evaluation and writing of the final version of the manuscript. M.M.S. designed and performed cell culture experiments together with A.I. A.Y. and T.S. assisted the cell culture experiments.

Acknowledgment

This work was supported by the EU-funded Marie Curie ITN 711 project PEPMIP (PITN-GA-2010-264699), the Marie Skłodowska-Curie Actions (H2020-MSCA-ITN-2016, 722171 Biocapture) and in part by the Deutsche Forschungsgemeinschaft DFG (Se 777/9-1). We are indepted to Prof. Dr. R. M. J. Liskamp, Utrecht University, for kind help and support with the synthesis of the phosphopeptide templates and to Alper Yılmaz and Thomas Sjöberg for assisting the binding tests and cell culture experiments. The authors are also grateful to Prof. Rainer Bischoff, University of Groningen, for valuable discussions. Proteomics and mass spectrometry research at SDU was supported by generous grants from the VILLUM Foundation to the VILLUM Center for Bioanalytical Sciences (Grant No. 7292 to O.N.J.) and from the Danish Ministry of Higher Education and Science to the research infrastructure PRO-MS: Danish National Mass Spectrometry Platform for Functional Proteomics (Grant No. 5072-00007B 720 to O.N.J.).

Experimental Section and Methods

Preparation of Imprinted Polymers. Bis-tetrabutylammonium (TBA) salts of Fmoc-YpYG-OMe, Fmoc-pYYG-OMe, Fmoc-YYG-OMe (each 0.5 mmol) or Fmoc-pYpYG-OMe (0.25 mmol), urea monomer (**1**) (1 mmol), and pentaerythritol triacrylate (PETA) (13.3 mmol) were dissolved in dry acetonitrile (MeCN) (6.1 mL). The initiator azobis 2,4-dimethyl)valeronitrile (ABDV) (1% w/w of total monomer) was added to the solution which was subsequently transferred to a glass ampoule, cooled to 0°C and purged with a flow of dry nitrogen for 5 min. The polymerization was then initiated by placing the tubes in a thermo-stated water bath pre-set at 50 ^{o}C overnight. After 24 h the tubes were broken, the polymers lightly crushed and then washed with MeOH:1N HCl (1:1/v:v) x 3 times and MeOH x 2 times for the removal of template. This was followed by sieving to isolate particle fractions between 25 μm and 50 μm for use in subsequent affinity enrichment tests.

Binding Test Using Model Peptides. Each polymer (10 mg) was suspended in 1.0 mL of equimolar GADDSYYTAR, GADDSYpYTAR, GADDSpYYTAR and GADDSpYpYTAR (each 20 μM) dissolved in MeCN:H2O at different ratios buffered with 0.1% TFA, FA or TEA or in different pH buffers . The suspensions were shaken vigorously for 2 h to promote binding equilibrium followed by centrifugation. The supernatant (500 μL) was dried and the sample reconstituted in H_2O/MeCN: 95/5 (0.1% TFA) (200 μL), and analyzed by reversed phase HPLC using a Prodigy 5 μm ODS-3 100 Å (Phenomenex, 150 x 4.6 mm) C18 column. Mobile phases were (A) 100% H_2O + 0.1% TFA and (B) 100% MeCN + 0.1 % TFA. A linear gradient method of 5% B to 20% B in 10 min at a flow rate of 1.5 mL/min was used. The injection volume was 100 μL and the

detection was performed by UV absorbance measurement at 275 nm. All experiments were performed in three parallel replicas.

Binding Isotherms. The imprinted polymers (10 mg) were separately suspended in 1 mL solution of different concentrations (0 – 100 μM) of the peptides (GADDSYYTAR, GADDSYpYTAR, GADDSpYYTAR, GADDSpYpYTAR) in MeCN/water: 90/10 (0.1% TFA) or in potassium phosphate (0.1M) buffer at pH = 7.4. The vials were shaken for 2 h followed by centrifugation and quantification of unbound analyte (C_{free}) by HPLC using the method described above. The amount of bound analyte per unit mass of polymer (*B*) was calculated according to equation 1 from the total peptide concentration (C_0), Cfree, volume (V) and polymer mass (m). The binding curves were then constructed by plotting *B* (μmol/g) against C_{free}, and were subsequently fitted using the GraphPad Prism 7 software (GraphPad Software, La Jolla, CA, USA) and the Langmuir mono-site binding model (2):

(1) $B = (C_0 - C_{free})\ V/m$

(2) $$B = B_{max} \cdot \frac{K_{eq} \cdot c}{1 + K_{eq} \cdot c}$$

where B_{max} is the maximum amount of solute bound by the polymer particles and K_{eq} the equilibrium constants.

Enrichments from spiked samples

MALDI TOF-MS analysis. A mixture of three of the model peptides (YY, YpY and pYpY or YY, pYY, and pYpY mixtures – each at spiking level: 1:5 (1 nmol of peptide mix: 5 nmol to digest) in a digest of BSA and β-casein followed by ZAP-70 MIPs enrichments. Solid phase extraction (SPE) was performed using a standard SPE cartridge packed with the MIP, MeCN/water 90/10 (0.1% TFA) as loading solvent (flow through), water (0.1% TFA) as washing solvent and

MeOH/water: 80/20 (0.1% TFA) followed by MeOH (0.1% TFA) as elution solvents. Three fractions as flow-through (FT), washing (W), and elution (E) were dried, redissolved and the peptide profile in each fraction was screened using a MALDI reflector time-of-flight mass spectrometer (Ultraflex mass spectrometer, Bruker-Daltonics GmbH, Bremen, Germany) equipped with a Scout-384 source in positive reflector mode. The residue was dissolved in 20% MeCN + 0.1% TFA (25 µL), then 1 µL of sample was mixed with 1 µL of matrix solution (2,5-dihydroxybenzoic acid, DHB (25.0 mg) was prepared in 1 mL of 50% MeCN and 1% phosphoric acid + 0.1% TFA) and deposited together on the target plate. The data collection was performed keeping scanning parameters constant for all samples. The spectra were collected by accumulating 2000 laser shots in the linear mode (relative laser focus: 50%). FlexControl software version 3.0 (Bruker Daltonics) was used for instrument control and data acquisition and further data processing was completed with the FlexAnaysis software version 3.0 (Bruker Daltonics).

LC MS/MS Analysis. ZAP70 deca-peptides were spiked in 12 protein digests (Carbonic anhydrase, BSA, Ovalbumin, Alpha casein, Beta casein, Beta lacto globulin, RNaseB, Alcohol dehydrogenase, Myoglobin, Transferrin, Lysozyme, Alpha amylase) with three different spiking level: 1:10 (1 pmol of peptide mix:10 pmol digest), 1:100 (100 fmol of peptide mix:10 pmol digest) and 1:1000 (10 fmol of peptide mix:10 pmol digest). Each solution was prepared in 90% MeCN + 0.1% TFA. The polymer particle (10 mg) was packed in single fritted SPE cartridges (ISOLUTE, Biotage) and was protected with a frit on top. In the enrichment protocol, the polymers were conditioned by using 90% MeCN + 0.1% TFA (3 x 1 mL) followed by loading the spiked solution (1 mL prepared by 90% MeCN + 0.1% TFA). The washing step was performed by using loading solution (2 x 0.5 mL) and 100% H_2O + 0.1% TFA (2 x 0.5 mL), lastly

the elution step was done by using two solutions, which were 80% MeOH + 0.1% TFA (0.5 mL) and 100% MeOH + 0.1% TFA (0.5 mL). In the regeneration, each SPE column was washed with following solutions: 80% MeOH + 20% HCl (0.1 M) (3 x 1 mL), 100% H_2O (3 x 1 mL), and 90% MeCN + 0.1% TFA (3 x 1 mL). Three fractions as loading (L), washing (W), and elution (E) were dried and elution fractions were used to test in LC-MS analysis. Each dried elution fraction for different spiking level with three replicas were tested in LC-MS analysis. Each fraction was firstly dissolved, vortexed and sonicated. The preparation of fraction for testing in LC-MS followed as: 1:100 elution fractions were dissolved in 18.8 µL in 0.1% FA (5.5 fmol/µL) and then 2 µL of the solution was diluted in 9 µL of loading solvent, 1:10 elution fractions were dissolved in 181.1 µL of 0.1% FA (5.5 fmol/µL) and then 2 µL of the solution was diluted in 9 µL of loading solvent (each dilution process was estimated as 1 fmol/µL peptides exist). Redissolved peptide samples were then analyzed on a Dione Ultimate 3000 RSLCnano system coupled online to an Orbitrap Fusion Tribrid mass spectrometer (Thermo Scientific). In the analysis of sample, approximately 10 fmol of each elution fraction was injected in 10 µL for 1 fmol/µL of peptides as expecting an elution of 100% recovery. This makes it possible to compare each elution fraction among each other. Additionally, two positive controls, which are 10.0 fmol injection of equimolar of ZAP70 peptides and 1:10 spiking solution in 10 fmol of ZAP70 peptides spiked in 100 fmol of protein digest, were analyzed. The LTQ-Orbitrap Velos was operated in positive ion mode with data-dependent acquisition. The full scan was acquired in the Orbitrap with an automatic gain control (AGC) target value of 1 × 106 ions and a maximum fill time of 500 ms. Full-MS scans were acquired with resolution of 60 000 fwhm followed by 10 MS/MS scans of the most intense ions, also acquired with a mass resolution at 15000 (HCD normalized collision energy = 35; activation time 10 ms). Raw data were viewed in Xcalibur v2.0.7 (Thermo Fisher Scientific, USA).

For in-gel digest experiments, the polymers were tested with peptide mixtures obtained from in-gel digests. In enrichment protocol, 4.0 mg of polymer was incubated with 200 μL of peptide mixture prepared in 90% MeCN + 0.1% TFA for 1 h., followed washing step using loading solution (200 μL) for 30 min. Both flow-through and washing fractions combined (FT+W). The elution was completed using first 50% MeOH + 0.1% TFA for 1 h. and then 80% MeOH + 0.1% TFA for 1 h. and then elution fractions (E) pooled together. Pre-enrichment, FT+W and E fractions were dried and analyzed by LC-MS/MS. The same LC-MS/MS analysis written above was done for profiling each fraction obtained by enrichment experiments.

Stimulation of cells and protein analysis. Jurkat (ATCC TIB-152) were cultured under conventional conditions (37°C, humidified atmosphere, containing 5% CO_2) in RPMI-1640 supplemented with 10% FCS (Gibco), sodium pyruvate (1 mM) and glucose (4.5 g/L), penicillin and streptomycin. Before stimulation, cells were serum starved for 3 hours before stimulation. Thereafter cells were sedimented at 300 x *g* for 5 min and resuspended at 3 x 10^6 cells/ml in RPMI-1640 without serum and stimulated with either anti-CD3 (mouse monoclonal, clone OKT3, Sigma-Aldrich, USA) at the indicated concentrations, anti-CD3 with 3% H_2O_2 (VWR, USA) and 3% H_2O_2 for 2 min at 37°C. To find out the optimal stimulation, cells were also stimulated with sodium orthovanadate (Sigma-Aldrich, Sweden) and sodium orthovanadate with 3% H_2O_2 for 15 min at 37°C. After stimulation, cells were immediately placed on ice, 1 ml ice-cold DPBS were added quickly before centrifugation at 300 x *g* for 5 min. The pellets were lysed for 30 min at 4°C with 150 µl lysis buffer (RIPA, Thermo Scientific, USA) including phosphatase inhibitor PhosSTOP (Sigma-Aldrich, USA) as well as protease inhibitor (Sigma-Aldrich, USA). Cellular debris were sedimented at 12 000 x *g* for 20 min at 4°C and supernatant harvested and stored at -80°C for subsequent studies. Quantitation of proteins were performed with

PierceTM BCA protein assay kit (Thermo Scientific, USA). SDS-PAGE and Western blotting were performed according to the manufacturer. Briefly, reduced SDS-PAGE was performed with Bio-Rad CriterionTM 12% respectively 7,5% TGX Stain-FreeTM Precast gels (Bio-Rad Laboratories, Hercules, CA) and proteins were transferred to 0,2 µm PVDF (Bio Rad, USA) using Trans-blot Turbo transfer pack, mini format Trans blot Turbo Transfer system (Bio Rad, USA), Mini-PROTEAN TGX (Bio Rad, USA). Thereafter membranes were blocked with 0,1% TBS-T with 5 % BSA for 60 min with agitation before incubation with Rabbit polyclonal antibodies to ZAP70 phospho Y493 (Abcam, Storbritannien), Rabbit monoclonal antibodies [EP2291Y] to ZAP70 phospho Y492 (Abcam, Storbritannien), and Anti-beta Actin antibodies (Abcam, Storbritannien). Antibody binding was detected with secondary antibodies Goat Anti-Rabbit IgG H&L (HRP) (Abcam, Storbritannien) and HRP Anti-beta Actin antibody (Abcam, Storbritannien) and enhanced via Clarity MaxTM Western ECL chemiluminescence (ECL) detection kit (Amersham, Buckinghamshire, Storbritannien). The ChemiDoc Imaging systems (Bio Rad, USA) were used for imaging.

In-gel Proteolytic Digest. 25 mM NH_4HCO_3 (100 mg/50 ml), 25 mM NH_4HCO_3 in 50% MeCN, 50% MeCN/5% formic acid, 12.5 ng/µL trypsin in 25mM NH_4HCO_3 were firstly prepared. Acrylamide gel was cut between 50 kDa to 75 kDA – where ZAP-70 phosphoprotein were detected- and gel was sliced into small pieces and placed into siliconized tubes. Gels were covered with 500 µL of 25 mM NH_4HCO_3 in 50% MeCN, vortexed for 15 min and the supernatant was discarded. This protocol was repeated twice. The gels were dried using Speed Vac. to complete dryness. The dried gels were then incubated with 200 µL of 10 mM DTT in 25 mM NH_4HCO_3 (1.5 mg/mL) for 1 h at 56°C. After reaction, the supernatant was removed and 200 µL of 55 mM iodoacetamide in 25 mM NH_4HCO_3 (10 mg/mL) was added. The reaction

allowed proceeding in the dark for 45 min at room temperature. Then, the supernatant was removed and the gel pellets were washed with 200 µL of 25 mM NH_4HCO_3 and vortexed for 15 min. This protocol was repeated three times and then the gels were dehydrated with 25 mM NH_4HCO_3 in 50% MeCN. The protocol was repeated twice and the gels were dried completely using Speed Vac. For the digestion, 100 uL of 12.5 ng/µL trypsin in 25mM NH_4HCO_3 was added and the tubes and placed on ice for 15 min for dehydration. Before incubation incubated at 37°C for 16 h, 200 µL of 25 mM NH_4HCO_3 in 50% MeCN was added and the samples. Thereafter, the solution was transferred to clean tubes and 100 µL of 50% MeCN/5% formic acid was added into gel pieces, vortexed for 30 min and the extracted digested pooled together. The in-gel digest protocol was repeated several times, pooled together and the extracted protein digest samples were concentrated.

References

1 Manning, G., Whyte, D. B., Martinez, R., Hunter, T. & Sudarsanam, S. The Protein Kinase Complement of the Human Genome. *Science* **298**, 1912-1934, doi:10.1126/science.1075762 (2002).

2 Johnson, S. A. & Hunter, T. Kinomics: methods for deciphering the kinome. *Nature Methods* **2**, 17-24 (2005).

3 Needham Elise, J., Parker Benjamin, L., Burykin, T., James David, E. & Humphrey Sean, J. Illuminating the dark phosphoproteome. *Science Signaling* **12**, eaau8645, doi:10.1126/scisignal.aau8645 (2019).

4 Ochoa, D. *et al.* The functional landscape of the human phosphoproteome. *Nature Biotechnology* **38**, 365-373, doi:10.1038/s41587-019-0344-3 (2020).

5 Carter, A. M. *et al.* Phosphoprotein-based biomarkers as predictors for cancer therapy. *Proceedings of the National Academy of Sciences* **117**, 18401, doi:10.1073/pnas.2010103117 (2020).

6 Thingholm, T. E., Jorgensen, T. J., Jensen, O. N. & Larsen, M. R. Highly selective enrichment of phosphorylated peptides using titanium dioxide. . *Nature Protoc.*, 1929–1935 (2006).

7 Riley, N. M. & Coon, J. J. Phosphoproteomics in the Age of Rapid and Deep Proteome Profiling. *Analytical Chemistry* **88**, 74-94, doi:10.1021/acs.analchem.5b04123 (2016).

8 Humphrey, S. J., Azimifar, S. B. & Mann, M. High-throughput phosphoproteomics reveals in vivo insulin signaling dynamics. *Nat Biotech* **33**, 990-995, doi:10.1038/nbt.3327

9 Bekker-Jensen, D. B. *et al.* Rapid and site-specific deep phosphoproteome profiling by data-independent acquisition without the need for spectral libraries. *Nature Communications* **11**, 787, doi:10.1038/s41467-020-14609-1 (2020).

10 Cheng, L. C., Tan, V. M., Ganesan, S. & Drake, J. M. Integrating phosphoproteomics into the clinical management of prostate cancer. *Clinical and Translational Medicine* **6**, e9, doi:https://doi.org/10.1186/s40169-017-0138-5 (2017).

11 Doll, S., Gnad, F. & Mann, M. The Case for Proteomics and Phospho-Proteomics in Personalized Cancer Medicine. *PROTEOMICS – Clinical Applications* **13**, 1800113, doi:https://doi.org/10.1002/prca.201800113 (2019).

12 Whiteaker, J. R. *et al.* Peptide Immunoaffinity Enrichment and Targeted Mass Spectrometry Enables Multiplex, Quantitative Pharmacodynamic Studies of Phospho-Signaling. *Molecular & cellular proteomics : MCP* **14**, 2261-2273, doi:10.1074/mcp.O115.050351 (2015).

13 Jeffrey, R. W. *et al.* A Multiplexed Mass Spectrometry-Based Assay for Robust Quantification of Phosphosignaling in Response to DNA Damage. *Radiation Research* **189**, 505-518, doi:10.1667/RR14963.1 (2018).

14 Whitcombe, M. J., Kirsch, N. & Nicholls, I. A. Molecular imprinting science and technology: a survey of the literature for the years 2004–2011. *Journal of Molecular Recognition* **27**, 297-401, doi:10.1002/jmr.2347 (2014).

15 Chen, L., Wang, X., Lu, W., Wu, X. & Li, J. Molecular imprinting: perspectives and applications. *Chemical Society Reviews* **45**, 2137-2211, doi:10.1039/C6CS00061D (2016).

16 Haupt, K. & Ayela, C. *Molecular Imprinting*. (Springer, 2012).

17 Sellergren, B. & Hall, A. J. in *Supramolecular Chemistry: from Molecules to Nanomaterials* (eds J. W. Steed & P. A. Gale) 3255-3282 (John Wiley & Sons Ltd, 2012).

18 Takeuchi, T. *et al.* Molecularly Imprinted Tailor-Made Functional Polymer Receptors for Highly Sensitive and Selective Separation and Detection of Target Molecules. *CHROMATOGRAPHY* **37**, 43-64, doi:10.15583/jpchrom.2016.007 (2016).

19 Cheong, W. J., Yang, S. H. & Ali, F. Molecular imprinted polymers for separation science: A review of reviews. *Journal of Separation Science* **36**, 609-628, doi:10.1002/jssc.201200784 (2013).

20 Haupt, K., Medina Rangel, P. X. & Bui, B. T. S. Molecularly Imprinted Polymers: Antibody Mimics for Bioimaging and Therapy. *Chemical Reviews* **120**, 9554-9582, doi:10.1021/acs.chemrev.0c00428 (2020).

21 Wulff, G., Gross, T. & Schönfeld, R. Enzyme models based on molecularly imprinted polymers with strong esterase activity. *Angew. Chem. Int. Ed. Engl.* **36**, 1962-9164 (1997).

22 Nishino, H., Huang, C.-S. & Shea, K. J. Selective protein capture by epitope imprinting. *Angewandte Chemie, International Edition* **45**, 2392-2396 (2006).

23 Hoshino, Y., Kodama, T., Okahata, Y. & Shea, K. J. Peptide Imprinted Polymer Nanoparticles: A Plastic Antibody. *J. Am. Chem. Soc. FIELD Full Journal Title:Journal of the American Chemical Society* **130**, 15242-15243 (2008).

24 Xing, R., Wen, Y., He, H., Guo, Z. & Liu, Z. Recent progress in the combination of molecularly imprinted polymer-based affinity extraction and mass spectrometry for targeted proteomic analysis. *TrAC Trends in Analytical Chemistry* **110**, 417-428, doi:https://doi.org/10.1016/j.trac.2018.11.033 (2019).

25 Emgenbroich, M. *et al.* A Phosphotyrosine-Imprinted Polymer Receptor for the Recognition of Tyrosine Phosphorylated Peptides. *Chem. Eur. J.* **14**, 9516-9529 (2008).

26 Shinde, S., Bunschoten, A., Kruijtzer, J. A., Liskamp, R. M. & Sellergren, B. Imprinted polymers displaying high affinity for sulfated protein fragments. *Angew Chem Int Ed Engl* **51**, 8326-8329, doi:10.1002/anie.201201314 (2012).

27 Chen, J. *et al.* Low-bias phosphopeptide enrichment from scarce samples using plastic antibodies. *Sci Rep* **5**, 11438, doi:10.1038/srep11438 (2015).

28 Yang, F., Lin, S. & Dong, X. An artificial receptor synthesized by surface-confined imprinting for the recognition of acetylation on histone H4 K16. *Chemical Communications* **51**, 7673-7676, doi:10.1039/C4CC09787D (2015).

29 Chen, J. *et al.* Validation of molecularly imprinted polymers for side chain selective phosphopeptide enrichment. *J Chromatogr A* **1471**, 45-50, doi:10.1016/j.chroma.2016.10.018 (2016).

30 Chen, Y., Li, D., Bie, Z., He, X. & Liu, Z. Coupling of Phosphate-Imprinted Mesoporous Silica Nanoparticles-Based Selective Enrichment with Matrix-Assisted Laser Desorption Ionization-Time-of-Flight Mass Spectrometry for Highly Efficient Analysis of Protein Phosphorylation. *Analytical Chemistry* **88**, 1447-1454, doi:10.1021/acs.analchem.5b04343 (2016).

31 Bllaci, L. *et al.* Phosphotyrosine Biased Enrichment of Tryptic Peptides from Cancer Cells by Combining pY-MIP and TiO2 Affinity Resins. *Anal Chem* **89**, 11332-11340, doi:10.1021/acs.analchem.7b02091 (2017).

32 Wierzbicka, C., Torsetnes, S. B., Jensen, O. N., Shinde, S. & Sellergren, B. Hierarchically templated beads with tailored pore structure for phosphopeptide capture and phosphoproteomics. *RSC Advances* **7**, 17154-17163, doi:10.1039/C7RA00385D (2017).

33 Incel, A. *et al.* Selective Enrichment of Histidine Phosphorylated Peptides Using Molecularly Imprinted Polymers. *Anal Chem* **93**, 3857-3866, doi:10.1021/acs.analchem.0c04474 (2021).

34 Shinde, S. *et al.* Urea-Based Imprinted Polymer Hosts with Switchable Anion Preference. *Journal of the American Chemical Society* **142**, 11404-11416, doi:10.1021/jacs.0c00707 (2020).

35 Chan, A. C., Irving, B. A., Fraser, J. D. & Weiss, A. The zeta chain is associated with a tyrosine kinase and upon T-cell antigen receptor stimulation associates with ZAP-70, a 70-kDa tyrosine phosphoprotein. *Proceedings of the National Academy of Sciences* **88**, 9166, doi:10.1073/pnas.88.20.9166 (1991).

36 Chan, A. C., Iwashima, M., Turck, C. W. & Weiss, A. ZAP-70: A 70 kd protein-tyrosine kinase that associates with the TCR ζ chain. *Cell* **71**, 649-662, doi:10.1016/0092-8674(92)90598-7 (1992).

37 Au-Yeung, B. B. *et al.* The structure, regulation, and function of ZAP-70. *Immunological Reviews* **228**, 41-57, doi:https://doi.org/10.1111/j.1600-065X.2008.00753.x (2009).

38 Wang, H. *et al.* ZAP-70: an essential kinase in T-cell signaling. *Cold Spring Harbor perspectives in biology* **2**, a002279-a002279, doi:10.1101/cshperspect.a002279 (2010).

39 Au-Yeung, B. B., Shah, N. H., Shen, L. & Weiss, A. ZAP-70 in Signaling, Biology, and Disease. *Annual Review of Immunology* **36**, 127-156, doi:10.1146/annurev-immunol-042617-053335 (2018).

40 Di Bartolo, V. *et al.* Tyrosine 319, a Newly Identified Phosphorylation Site of ZAP-70, Plays a Critical Role in T Cell Antigen Receptor Signaling *. *Journal of Biological Chemistry* **274**, 6285-6294, doi:10.1074/jbc.274.10.6285 (1999).

41 Visco, C. *et al.* Activation of Zap-70 Tyrosine Kinase Due to a Structural Rearrangement Induced by Tyrosine Phosphorylation and/or ITAM Binding. *Biochemistry* **39**, 2784-2791, doi:10.1021/bi991840x (2000).

42 Mège, D. *et al.* Mutation of Tyrosines 492/493 in the Kinase Domain of ZAP-70 Affects Multiple T-cell Receptor Signaling Pathways *. *Journal of Biological Chemistry* **271**, 32644-32652, doi:10.1074/jbc.271.51.32644 (1996).

43 Klammt, C. *et al.* T cell receptor dwell times control the kinase activity of Zap70. *Nature Immunology* **16**, 961-969, doi:10.1038/ni.3231 (2015).

44 Huber, R. G., Fan, H. & Bond, P. J. The Structural Basis for Activation and Inhibition of ZAP-70 Kinase Domain. *PLOS Computational Biology* **11**, e1004560, doi:10.1371/journal.pcbi.1004560 (2015).

45 Hall, A. J. *et al.* Urea Host Monomers for Stoichiometric Molecular Imprinting of Oxyanions. *Journal of Organic Chemistry* **70**, 1732-1736 (2005).

46 Wulff, G. & Knorr, K. Stoichiometric imprinting. *Bioseparation* **10**, 257 (2002).

47 Chan, W. C. & White, P. D. *Fmoc solid phase peptide synthesis*. (Oxford University Press, USA, 2000).

48. We noted during data analysis that the sample spiked with YY+YpY+pYpY was contaminated with pYY. The contamination originates from impure YpY estimated to contain ca 88% YpY and the rest pYY. As seen in Fig. 3a and Fig. S23a, presence of this impurity adds to illustrate the high sequence specificity of the polymers.

49 Lysechko, T. L. & Ostergaard, H. L. Differential Src Family Kinase Activity Requirements for CD3ζ Phosphorylation/ZAP70 Recruitment and CD3ε Phosphorylation. *The Journal of Immunology* **174**, 7807, doi:10.4049/jimmunol.174.12.7807 (2005).

50 Natarajan, V., Vepa, S., Verma, R. S. & Scribner, W. M. Role of protein tyrosine phosphorylation in H2O2-induced activation of endothelial cell phospholipase D. *American Journal of Physiology-Lung Cellular and Molecular Physiology* **271**, L400-L408, doi:10.1152/ajplung.1996.271.3.L400 (1996).

51 Tessier, S., Chapdelaine, A. & Chevalier, S. Effect of vanadate on protein phosphorylation and on acid phosphatase activity in the canine prostate. *Molecular and Cellular Endocrinology* **64**, 87-94, doi:https://doi.org/10.1016/0303-7207(89)90068-3 (1989).